I wish to thank the referee for his helpful comments on the first manuscript of this note.

APPENDIX

The best-plane calculation is conveniently referred to a Cartesian system with origin at the centroid of the group of atoms involved, and with axes directed along the eigenvectors of a matrix which has the same functional form as that of the tensor of inertia (*e.g.* Rollett, 1965). Denoting the unit vectors of this Cartesian system by $\hat{v}_1$, $\hat{v}_2$, $\hat{v}_3$ and the crystal and reciprocal-lattice basis vectors by a_1, a_2, a_3 and a_1^*, a_2^*, a_3^* respectively, we can express an atomic position vector as

$$\mathbf{r} = \sum_k X_k^I \hat{v}_k = \sum_l x_l^{cc} \mathbf{a}_l, \qquad (A1)$$

where X_k^I, $k = 1, 2, 3$, are Cartesian coordinates, referred to the best-plane system and x_l^{cc}, $l = 1, 2, 3$, are fractional coordinates, referred to the centroid of the group as origin and to the crystal system.

We further have the scalar products

$$\mathbf{r} \cdot \hat{v}_p = \sum_k X_k^I \hat{v}_k \cdot v_p = \sum_k X_k^I \delta_{kp} = X_p^I \qquad (A2)$$

and

$$\mathbf{r} \cdot \mathbf{a}_p^* = \sum_l x_l^{cc} \mathbf{a}_l \cdot \mathbf{a}_p^* = \sum_l x_l^{cc} \delta_{lp} = x_p^{cc} \qquad (A3)$$

since v_k are orthonormal and a_l and a_p^* are mutually reciprocal sets of basis vectors.

In any such calculation we evaluate or have access to the following transformation relating the crystal and the best-plane systems

$$X_k^I = \sum_l R_{kl} x_l^{cc}. \qquad (A4)$$

Comparing (A2) and (A3) with (A4) it is seen that the rows of the matrix **R** contain the components of the vectors $\hat{v}_k$, $k = 1, 2, 3$, referred to the reciprocal vectors $\mathbf{a}_1^*$, $\mathbf{a}_2^*$ and $\mathbf{a}_3^*$. One of the $\hat{v}$ vectors corresponds to the plane normal, and its representation, required for evaluating the perpendicular variances, discussed in the text, is thus a by-product of a conventional best-plane calculation.

References

CRAMÉR, H. (1951). *Mathematical Methods of Statistics.* Princeton Univ. Press.
CRUICKSHANK, D. W. J. (1967). In *International Tables for X-ray Crystallography*, Vol. II. Birmingham: Kynoch Press.
LINNIK, J. W. (1961). *Methode der Kleinsten Quadrate in Moderner Darstellung.* Berlin: Deutscher Verlag der Wissenschaften.
PATTERSON, A. L. (1967). In *International Tables for X-ray Crystallography*, Vol. II. Birmingham: Kynoch Press.
ROLLETT, J. S. (1965). *Computing Methods in Crystallography.* Oxford: Pergamon Press.
SHAANAN, B. & SHMUELI, U. (1980). *Acta Cryst.* B36, 2076–2082.
SHMUELI, U. & GOLDBERG, I. (1974). *Acta Cryst.* B30, 573–578.

Hydrocarbon Chain Disorder in C-phase Potassium Caprate and its Associated Diffuse Scattering

BY D. M. GLOVER*

Department of Physics, The University of Birmingham, Birmingham B15 2TT, England

Abstract

Structural studies of the crystalline monoclinic C phase of the potassium soap $K^+ . C_{10}H_{19}O_2^-$ (space group $P2_1/a$, $a = 8.145 \pm 0.044$, $b = 5.726 \pm 0.010$, $c = 28.309 \pm 0.061$ Å, $\beta = 94°35' \pm 46'$, $Z = 4$) stable above 349 K are reported. Analysis of the Bragg diffraction data demonstrates that the heavy end group and the first four carbon atoms in the hydrocarbon chain, C(1) to C(4), retain the ordered configuration of the room-temperature A phase. The remainder of the chain, C(5) to C(10), is disordered. The disordered segments of chain adopt an average parallel packing on

* Present address: Cavendish Laboratory, Madingley Road, Cambridge, CB3 0HE, England.

0567-7394/81/020251-13$01.00

a pseudo-hexagonal lattice. The chain axes are approximately parallel to the inter-layer long spacing $d(001)$. It is proposed that the disorder is due to rotational isomerism about the bonds between atoms C(3) and C(4), C(5) and C(6), C(7) and C(8). This model is consistent with available thermodynamic data. Strong X-ray diffuse scattering associated with, and extending between, the reciprocal-lattice points $20l$ and $11l$ has been observed from the C-phase soap. This diffuse scattering is interpreted in terms of the proposed disorder. The localization of the diffuse scattering about the specified lattice points is accounted for by the presence of intermolecular correlations.

1. Introduction

This paper reports the results of structural studies of the C phase of potassium caprate $K^+.C_{10}H_{19}O_2^-$ which is stable above 349 K. It is well established that the alkali metal soaps of the general formula $MC_nH_{2n-1}O_2$ (abbreviated to MC_n in the following) exhibit complex polymorphism (Gray & Winsor, 1974). Each soap undergoes a series of phase transitions between the crystalline form, stable at low temperatures, and the isotropic liquid which occurs above the melting point. The structures of the various phases have been characterized using X-ray powder techniques by Lomer (1952), Skoulios & Luzzati (1961) and Gallot & Skoulios (1966a,b,c, 1968).

Lomer studied potassium soaps with n ranging from 8 to 18. At room temperature all the soaps in the series are crystalline. KC_8 and KC_{10} adopt the monoclinic A-phase structure and the others the triclinic B-phase structure. All the soaps transform to the crystalline monoclinic C phase at temperatures between 323 and 373 K. Similar transitions are observed in the soaps of the other alkali metals.

The A/B to C transition is accompanied by an abrupt narrowing of the proton magnetic resonance (PMR) line in the nuclear magnetic resonance (NMR) spectra of the soaps (Grant & Dunell, 1960, 1961; Janzen & Dunell, 1962). This indicates that a marked increase in the extent of motion of the hydrocarbon chain component of the soap molecules occurs at the transition.

It is known that in the A- and B-phase potassium soaps the chains are in the fully extended all-*trans* configuration. A well refined structure for the A phase of KC_{10} has been given by Lewis & Lomer (1969). This structure is illustrated schematically in Fig. 1. It is monoclinic with space group $P2_1/a$ and contains four molecules per unit cell. The chains adopt a crossed-chain structure when projected down the a axis. They cross each other at an angle of about 60°. The potassium and carboxyl ions form double ionic sheets with the potassium ions of one sheet approximately

opposite the carboxyl groups of the other sheet and *vice versa*.

Although the unit-cell dimensions and space group of C-phase KC_{10} are known (Lomer, 1952) no details of the crystal structure have yet been reported. Two previous attempts to determine the structure from single-crystal X-ray diffraction data have been made (Dumbleton, 1964; Lewis, 1967, 1968). These demonstrated that the packing of the ionic layer and probably that of the first four carbon atoms in the chain [C(1) to C(4), numbering from the carboxyl group] is similar to that in the A phase. However, despite much careful and detailed work all attempts to locate a physically realistic, ordered configuration for the remainder of the chain failed.

In the light of the PMR result, which suggests that in the C phase at least part of the hydrocarbon chain is in a highly mobile or 'partially fluid' state, the Bragg diffraction data collected by Lewis has been re-examined. Further insight into the physical state of the chains has been obtained from examination of the possible modes of packing for disordered chains in KC_{10}. On the basis of these investigations a model for the structure is proposed. In addition, a study of the diffuse scattering of X-rays from a single crystal of C-phase KC_{10} has been made. The scattering observed is interpreted in terms of the proposed structure.

2. Analysis of the Bragg diffraction data

Lewis (1967, 1968) collected Bragg diffraction data from a single crystal of KC_{10} which had been heated
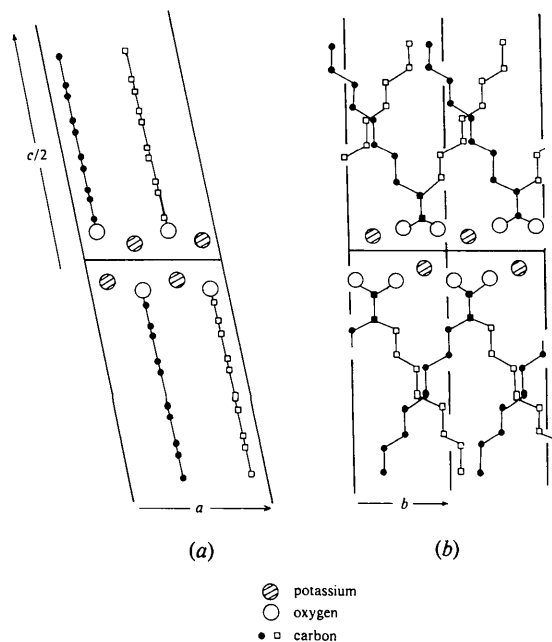

Fig. 1. The structure of A-phase KC_{10} (Lewis & Lomer, 1969): (a) b-axis projection; (b) a-axis projection.

through the transition in a stream of hot nitrogen. Three-dimensional electron density distributions, calculated using Lewis's data phased from the potassium, oxygen and first three carbon atoms, show the chain from C(4) onwards as a diffuse cylinder of electron density with its axis lying approximately along the line $x = z/4 + 0.125$, $y = 0.5$. Individual atoms are not resolved for this part of the chain. In structure factor calculations the value of R (where $R = \sum \Delta F_o / \sum |F_o|$) is minimized when the remaining seven carbon atoms are placed, with large temperature factors, on or close to this line (Glover, 1977).

Projections of the electron density distribution down the a and b axes are given in Fig. 2. Signs for the structure factors used to calculate these projections were determined from a set of atomic coordinates in which atoms C(4) to C(10) were located as described.* R for this data was 0.23 but it is not suggested that the tabulated coordinates and temperature factors are significant in giving a physical interpretation of the distribution of scattering matter within the unit cell.

---

* These coordinates and isotropic thermal parameters, together with a list of structure factors, have been deposited with the British Library Lending Division as Supplementary Publication No. SUP 35725 (6 pp.). Copies may be obtained through The Executive Secretary, International Union of Crystallography, 5 Abbey Square, Chester CH1 2HU, England.
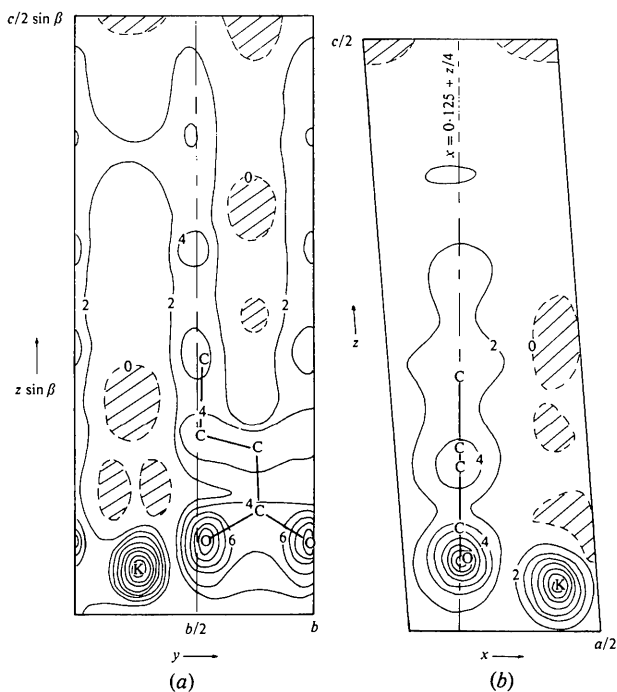
It is not possible to conceive of a single ordered configuration of the chain, with physically realistic values for bond lengths and angles such that the atoms C(4) to C(10) all lie in a straight line. It is proposed that this portion of the chain is dynamically disordered amongst several alternative configurations. Within one layer the disordered segments are on average parallel and adopt a pseudo-hexagonal packing arrangement (Fig. 18).

3. Molecular packing in C-phase KC_{10}

For chain molecules, angles of rotation about interatomic bonds permit a diversity of molecular configurations or 'conformations' (Flory, 1969). In C-phase KC_{10} the first four carbon atoms retain the minimum-energy all-*trans* conformation generally found in the crystalline state. The PMR results and electron density distribution suggest that the remainder of the chain is in the mobile 'liquid-like' state characteristic of chain molecules in liquid-crystalline phases. In this state the chains are statistically distributed amongst the various rotational isomers produced by rotations of $\pm 120°$ ('*gauche*' conformations) from the *trans* conformation (Lee, 1975).

Steric interactions between neighbouring molecules will restrict the possible rotational isomers in C-phase KC_{10}. Molecular packing models were therefore examined in order to determine which rotational isomers can exist within the limits of the unit cell.

The a-axis projection of an idealized model for the chain packing in A-phase KC_{10} is illustrated in Fig. 3. In the structure given by Lewis & Lomer (1969) the chain is distorted from this ideal situation, but the model given serves as a useful starting point.

Fig. 2. Projections of the electron density of C-phase KC_{10} down a and b. The contours are labelled in units of e Å^{-2}. The atomic sites of the potassium, oxygen and ordered carbon atoms in the asymmetric unit have been marked: (a) a-axis projection; (b) b-axis projection.
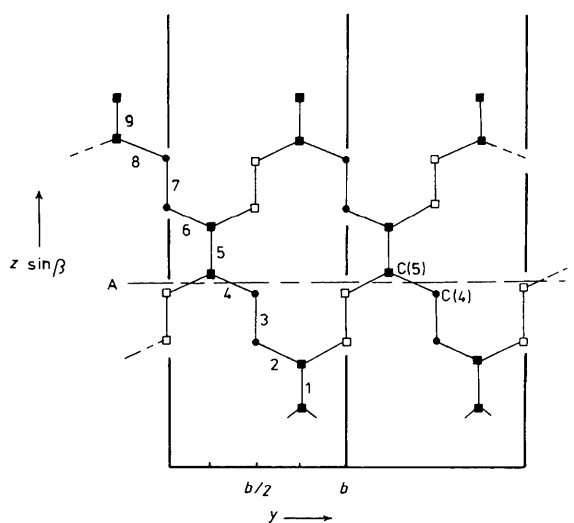

Fig. 3. The a-axis projection of an idealized chain packing mode for A-phase KC_{10}. The odd-numbered bonds are parallel to the long spacing $d(001)$.

In the *C* phase the first four carbon atoms retain the ordered all-*trans* configuration. Rotations may be introduced about bonds 3 to 9 of Fig. 3 without altering the configuration of atoms C(1) to C(4). The long spacing $d(001)$ changes little at the transition, increasing by approximately 2%. This implies that rotations take place only about the vertical odd-numbered bonds of Fig. 3 and not about the non-vertical even-numbered bonds.

Examinations of scale packing models demonstrates that the suppression of rotations about non-vertical bonds results from steric interactions between neighbouring molecules. A vertical bond in a given molecule is parallel to the corresponding bonds in its nearest-neighbour molecules and it is possible for cooperative rotations to take place about these bonds without causing severe steric overlap. Fig. 4(*a*) shows the cross section taken through the line *AB* of Fig. 3. The molecular envelopes have been constructed using values for bond lengths and van der Waals radii given by Kitaigorodsky (1957). In Fig. 4(*b*) *gauche* rotations have been introduced about bond 3 and one possible packing arrangement for this section of the molecule is shown. The *y* coordinates of atoms C(4) have been allowed to relax slightly from those in Fig. 3 to permit efficient packing.
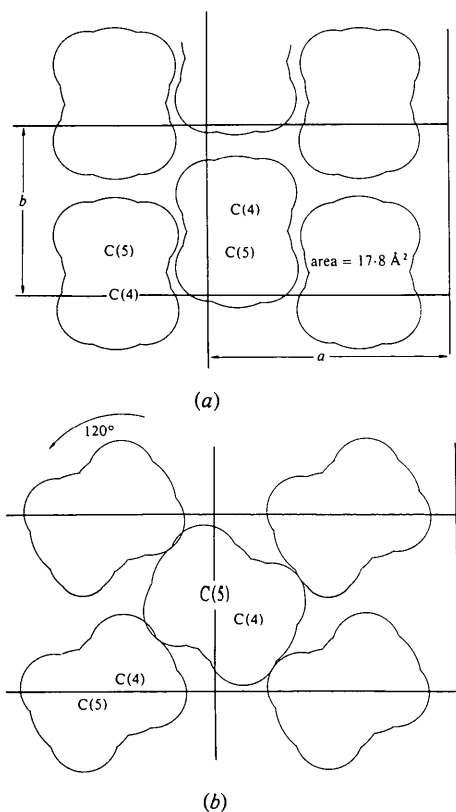
A *gauche* conformation about a non-vertical bond reduces the effective length of the molecule perpendicular to the ionic sheets. It must, therefore, for a molecule of fixed volume, give rise to an increase in the effective cross-sectional area of the molecule parallel to these sheets at some point along its length. The cross-sectional area available to each molecule in the *ab* plane is given by $(a \times b)/2 = 23 \cdot 32$ Å^2. The area of each of the molecular sections in Fig. 4(*b*) is $17 \cdot 8$ Å^2. In Fig. 5 the cross section parallel to the *ab* face of the unit cell through a $2g1$ kink (successive rotations of $+120°$ and $-120°$ about parallel bonds) formed about non-vertical bonds is shown. This has an area of $29 \cdot 2$ Å^2. The suppression of rotations about the non-vertical bonds can thus be interpreted as arising from steric hindrance resulting from the increase in effective cross-sectional area accompanying such rotations. In the *C*-phase soap the ionic layers remain crystalline and the area of the *ab* face of the unit cell is presumably determined by the atomic arrangement of these tightly bound layers.

Thus, molecular packing considerations indicate that the rotational isomerism introduced at the phase transition can involve conformational changes about only bonds 3, 5, 7 and 9 of Fig. 3. There is some evidence from thermodynamic measurements (Lomer, 1977) and from NMR studies (Janzen & Dunell, 1962) that the methyl end groups are already reorientating in *A*-phase KC_{10}. We therefore conclude that just three bonds, 3, 5 and 7, are involved in the transition. Detailed examination of packing models confirms that, provided there is a considerable degree of correlation between the states of neighbouring molecules, rotational isomers produced by introducing *gauche* conformations about these three bonds may exist within the *C*-phase unit cell without giving rise to severe steric overlap.

Some support for this model is provided by thermodynamic measurements (Glover & Lomer, 1979). The measured value for the entropy change at the transition was $23 \cdot 5 \pm 0 \cdot 6$ J K^{-1} mol^{-1}. In the absence of intermolecular interactions the configurational entropy change, ΔS_c, associated with the proposed disorder was estimated to be $25 \cdot 8$ J K^{-1}

(*a*)

(*b*)

Fig. 4. Hydrocarbon chain packing in KC_{10}. (*a*) Cross section through the line *AB* of Fig. 3. (*b*) As (*a*) but with *gauche* conformations about bond 3 of Fig. 3.
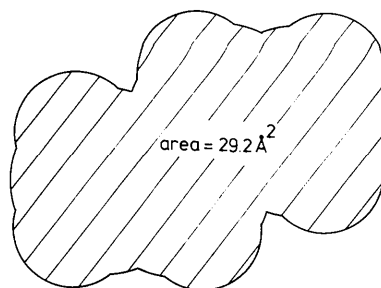

Fig. 5. Cross section parallel to the *ab* face of the unit cell through a $2g1$ kink formed about 'non-vertical' bonds.

mol^{-1}. This calculated value would be reduced by the presence of short-range order or correlations between the conformation of neighbouring molecules, perhaps substantially so, but it is at least plausible that the configurational entropy associated with the disordering of the chains is the dominant contribution to the total entropy change at the transition.

In Fig. 6 the a-axis projection of all the 27 possible configurations of the molecule (three conformations per bond for three bonds) has been drawn for a single molecule starting from the all-*trans* configuration shown in Fig. 3. The weights given to the atomic sites have been calculated assuming equal probability for each of the 27 alternatives. In the electron density map for this projection, Fig. 2(a), the chain appears to be on average concentrated near the line $y = 0.5$. This suggests that kinked chain configurations with two or three *gauche* bonds which orient the chain along this line are more probable relative to the more extended all-*trans* and one *gauche* configurations than they would be if weighted solely on the basis of their intramolecular energies. Adoption of an average orientation of the chain axis along the line $y = 0.5$, $x = z/4 + 0.125$ gives rise to the pseudo-hexagonal parallel packing of the disordered parts of the chain shown in
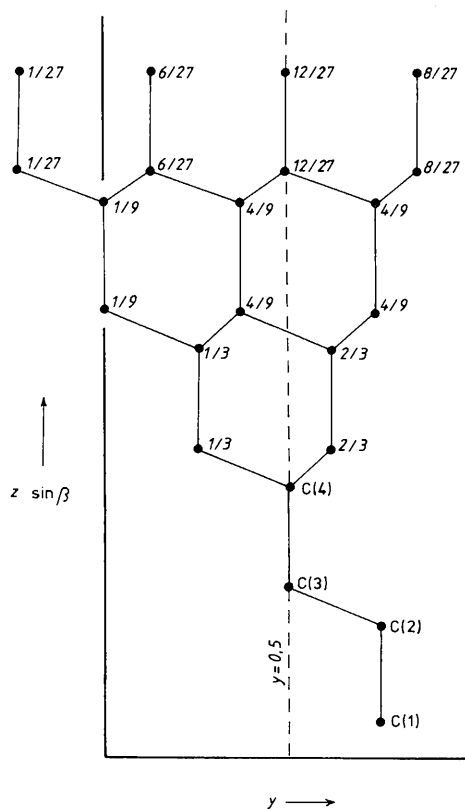

Fig. 6. The a-axis projection of all 27 possible configurations of the hydrocarbon chain of a single molecule produced by *gauche* conformations about bonds 3, 5 and 7 of Fig. 3.

Fig. 18. The more extended chain configurations which deviate most from this parallel packing arrangement will have on average a more unfavourable steric interaction with neighbouring molecules than kinked configurations.

4. The diffuse scattering of X-rays from C-phase KC_{10}

Theoretical

The total X-ray intensity $I(s)$ diffracted by a crystal exhibiting structural disorder contains a diffuse component with a structure determined by the nature of the disorder. General theoretical treatments of the diffuse scattering due to structural imperfections have been given by Zachariasen (1945), Matsubara (1952), Wilson (1962) and Cochran (1956).

In the following, Fourier techniques are used in order to derive a general expression for the diffuse scattering from a crystal with constant lattice parameters but variable unit cells, the situation which occurs in the structure proposed for C-phase KC_{10}.

A fundamental result of diffraction theory is that the scattered intensity from a distribution of electron density $\rho(\mathbf{r})$ is equal to the Fourier transform (FT) of the self-correlation or 'Q' function of the electron density (Hosemann & Bagchi, 1962; Amorós & Amorós, 1968).

Consider a crystal consisting of N unit cells. $Q(\mathbf{r})$ is given by

$$Q(\mathbf{r}) = \int \sum_m^N \rho_m(\mathbf{r}' - \mathbf{u}_m) \sum_{m'}^N \rho_{m'} (\mathbf{r}' - \mathbf{u}_{m'} + \mathbf{r}) \, dv', \qquad (1)$$

where $\rho_m(\mathbf{r})$ is the electron density of the mth unit cell and $\mathbf{u}_m$ is the lattice vector connecting the origin to the unit cell m.

When N is large (1) corresponds to the sum of N terms on each of N' lattice points ($N' \simeq 8\,N$ for a three-dimensional crystal with large N).

If there are n types of unit cell then, if P_i is the probability that a given unit cell is of the type i and $p(ij\mathbf{a})$ is the conditional probability that if a given unit cell is of type i then a unit cell separated by the vector $\mathbf{a}$ is of type j, (1) reduces to

$$Q(\mathbf{r}) = N \sum_m^{N'} \left\{ \left[\sum_i^n \sum_j^n P_i p(ij\mathbf{u}_m) \, Q_{ij}(\mathbf{r}) \right] * \delta(\mathbf{r} - \mathbf{u}_m) \right\}, \qquad (2)$$

where $Q_{ij}(\mathbf{r})$ is the 'image' (Buerger, 1962) of a unit cell type i on a unit cell type j.

The Q function of the hypothetical average crystal is given by

$$Q_{av}(\mathbf{r}) = N \left(\sum_i^n \sum_j^n P_i P_j Q_{ij}(\mathbf{r}) \right) * \sum_m^{N'} \delta(\mathbf{r} - \mathbf{u}_m). \qquad (3)$$

Adding and subtracting this to the right-hand side of (2) we have

$$Q(\mathbf{r}) = Q_{av}(\mathbf{r}) + N \sum_{m}^{N'} \left(\left\{ \sum_{i}^{n} \sum_{j}^{n} P_i[p(ij\mathbf{u}_m) - P_j] \right. \right.$$
$$\left. \left. \times Q_{ij}(\mathbf{r}) \right\} * \delta(\mathbf{r} - \mathbf{u}_m) \right) \qquad (4)$$
$$= Q_{av}(\mathbf{r}) + Q_D(\mathbf{r}).$$

Thus

$$I(\mathbf{s}) = \mathrm{FT}\ Q(\mathbf{r}) = \mathrm{FT}\ Q_{av}(\mathbf{r}) + \mathrm{FT}\ Q_D(\mathbf{r}). \qquad (5)$$

The Fourier transform of $Q_{av}(\mathbf{r})$ gives the Bragg scattering which is the same as that given by the average crystal structure. The diffuse scattering $I_D(\mathbf{s})$ is given by the Fourier transform of $Q_D(\mathbf{r})$.

Re-arranging (5) we have

$$I_D(\mathbf{s}) = \mathrm{FT}\ Q(\mathbf{r}) - \mathrm{FT}\ Q_{av}(\mathbf{r}) \qquad (6)$$

or

$$\mathrm{FT}\ I_D(\mathbf{s}) = Q(\mathbf{r}) - Q_{av}(\mathbf{r}). \qquad (7)$$

Equation (6) is the general result given by Amorós & Amorós (1968). The diffuse scattering is given by the difference between the Fourier transform of the Q function of the actual crystal and that of the average crystal. Equation (7) states that the Fourier transform of the diffuse scattering is equal to the difference between the Q functions of the average and actual crystals. This relationship provides a basis for the interpretation of experimentally observed structural diffuse scattering. This 'difference Q function' will contain both positive and negative regions. The positive regions originate from interatomic vector displacements weighted more strongly in the real crystal than in the average crystal. The negative regions originate from displacements weighted more strongly in the average crystal than in the real crystal.
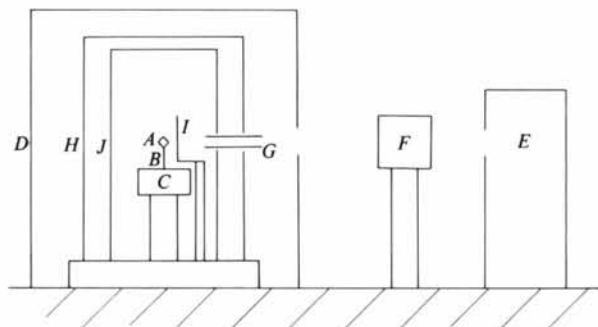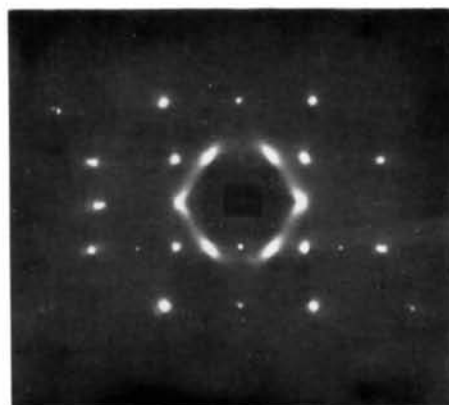
Experimental

The reciprocal space of C-phase KC_{10} was surveyed for diffuse X-ray scattering attributable to the proposed molecular disorder using a photographic technique. A schematic diagram of the apparatus is given in Fig. 7. Single crystals of KC_{10} prepared by the method described by Lewis & Lomer (1969) were mounted along their b axis in the goniometer. Heat was supplied to the crystal from an adjacent electrically heated wire. The temperature was monitored by a copper/constantan thermocouple which also served as the mount for the crystal. Temperature calibration was effected by observing the fusion of small samples of substances with well defined melting points. As a result of temperature fluctuations and the existence of temperature gradients across the specimen, temperature control was no better than ± 5 K. This degree of control was, however, quite adequate to ensure that the crystal was maintained in a given phase for the duration of an exposure.

To reduce unwanted air scatter the goniometer assembly was placed in a vacuum chamber. Background scattering was further reduced by placing a 12 μm sheet of aluminium foil between the crystal and the

(a)

Fig. 7. Schematic diagram of the apparatus used for the diffuse scattering studies: A crystal; B copper/constantan thermocouple; C goniometer head; D vacuum chamber; E X-ray source; F LiF monochromator crystal; G collimator; H film holder; I hot wire; J fluorescent radiation filter.
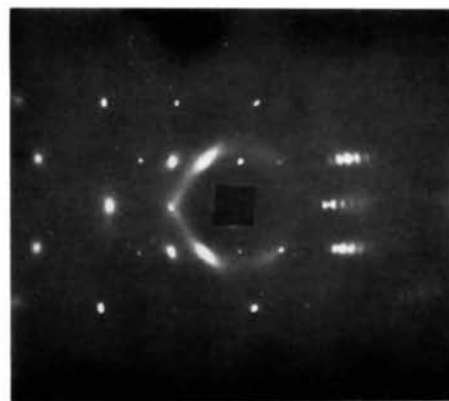
(b)

Fig. 8. Diffraction patterns recorded from a single crystal of KC_{10} at 373 K. (a) $\varphi = 0°$; (b) $\varphi = 30°$.

film. This served as a filter for fluorescent X-rays from the potassium atoms in the soap. X-rays from a copper target in the generator (Philips type PN 1009/30) were monochromatized by reflection from a doubly bent lithium fluoride single crystal. The reflection angle of the monochromator crystal was set to select the copper $K\alpha$ component of the incident X-ray spectrum. The X-ray set was run at 40 kV and 20 mA for all exposures.

With a collimator with beam-defining apertures of 1·0 and 0·5 mm and with exposure times of 5 to 10 h, trial photographs demonstrated that strong diffuse scattering, highly localized in reciprocal space, appeared at the transition from the A to the C phases. The distribution of this diffuse scattering was surveyed with a series of photographs in which the angle φ between the incident beam and the c^* axis was altered in steps of 10°. This series of exposures was taken from one crystal, the temperature of which was maintained at 373 K throughout the experiment. All films were developed simultaneously. For purposes of comparison a similar set of diffraction patterns was recorded at room temperature from a crystal in the A phase.
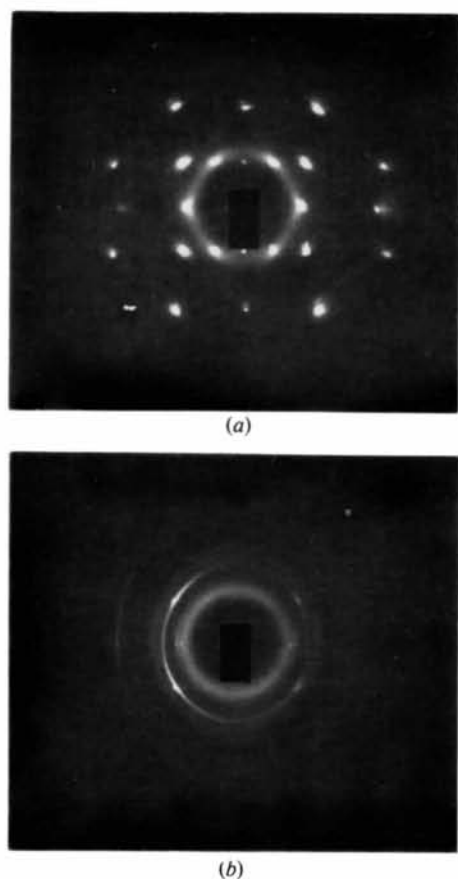
Results

Two of the photographs recorded from C-phase KC_{10} are reproduced in Fig. 8. The principal feature of these photographs is the strong diffuse scattering associated with and streaked diagonally between lattice points $11l$ and $20l$, $\bar{1}1l$ and $\bar{2}0l$ and the points related to these by the centre of symmetry at the origin. These diffuse streaks did not appear on any of the photographs taken with the crystal in the A phase. Diffuse scattering associated with, and extending in the b^* direction between, particular lattice points was common to both phases, as were somewhat weaker diffuse streaks in the a^* direction and more extensive diffuse regions observed with φ close to 90°.

Comparison of the two sets of photographs showed that the diagonal streaks described were the only additional diffuse scattering features present in the higher-temperature phase. These were considerably more intense than all other diffuse scattering features. The temperature dependence of these diagonal streaks was investigated with a series of photographs taken from a crystal oriented at $\varphi = 0°$.

The temperature was increased by ~40 K between successive exposures. Within the accuracy available from the visual comparison of photographic data, the spatial distribution and the intensity of the diffuse scattering characteristic of C-phase KC_{10} was found to be independent of temperature at least up to 456 K. Between 491 and 513 K (Fig. 9) a further transition was observed. At 491 K the higher-angle reflections of the C phase were weaker and the diffuse streaks had become more ring-like in character. At 513 K the diffuse region had become a complete ring as had the Bragg reflections although these were still preferentially

(a)

(b)

Fig. 9. Diffraction patterns recorded from a single crystal of KC_{10} oriented at $\varphi = 0°$. (a) 491 K; (b) 513 K.

Fig. 10. Diffuse scattering from C-phase KC_{10} in the section of reciprocal space perpendicular to $\mathbf{c}^*$ passing through the origin. The contours are labelled in relative units.

oriented as in the original crystal. Grant & Dunell (1961) reported that the final narrowing of the NMR line from KC_{10} to within the limits of their spectrometer's resolution was completed at 522 K.

Maps showing the distribution in reciprocal space of the diffuse scattering characteristic of C-phase KC_{10} are given in Figs. 10 and 11. The contours of equal diffuse intensity on these figures were plotted from microdensitometer scans of the photographs. Fig. 10 represents the section of reciprocal space perpendicular to c^* and passing through the origin. The diffuse intensity at the reciprocal-lattice points was estimated by extrapolation according to a theory of the origin of the diffuse streaks (Appendix).

Interpretation of the diffuse scattering

The Fourier transform of Fig. 10 is given in Fig. 12. The transformation was performed by summing a Fourier series at each of the points on a two-dimensional grid in real space. Fourier coefficients were obtained from the microdensitometer scans used to construct Fig. 10. The diffuse intensity was measured at points on a grid in reciprocal space of spacing $a^*/6$ in the direction parallel to a^* and $b^*/18$ in the b^* direction. 276 coefficients were included in the summations. A complete repeating unit of the Fourier synthesis was plotted to check that no overlap of the repeated function had occurred. Corrections for polarization, divergence and absorption were not made as for the purposes of this work they were assumed to be small. A trial transformation based on a coarser grid with just 66 coefficients included produced essentially the same result as that given by Fig. 12, despite intensity differences of up to 50% from those in the later, more carefully performed transformation.

Fig. 12 is the projection of the difference Q function of C-phase KC_{10} down the interlayer long spacing $[d(001)]$ on to the ab section of real space. The symmetry of this function is the same as that of the function transformed in order to obtain it. The positive peak at the origin is expected for any disordered structure. The interpretation of the other features is best approached by reference to models for the disorder in C-phase KC_{10}.

Fig. 11. Diffuse scattering from C-phase KC_{10} in sections of reciprocal space perpendicular to b^*. (a) Zero layer; (b) $\frac{1}{2}b^*$ layer; (c) b^* layer.

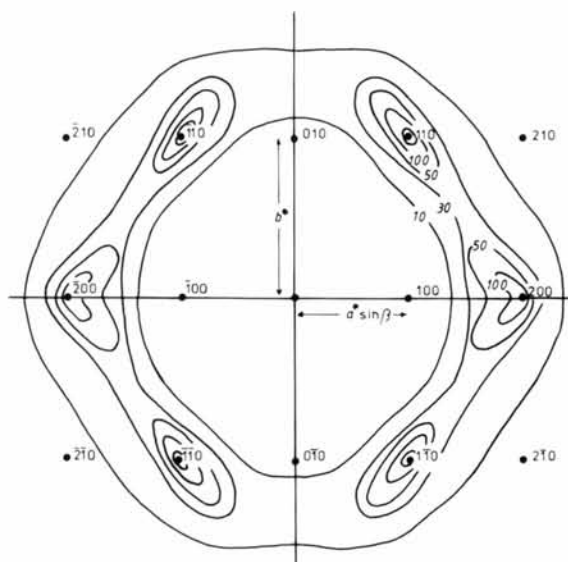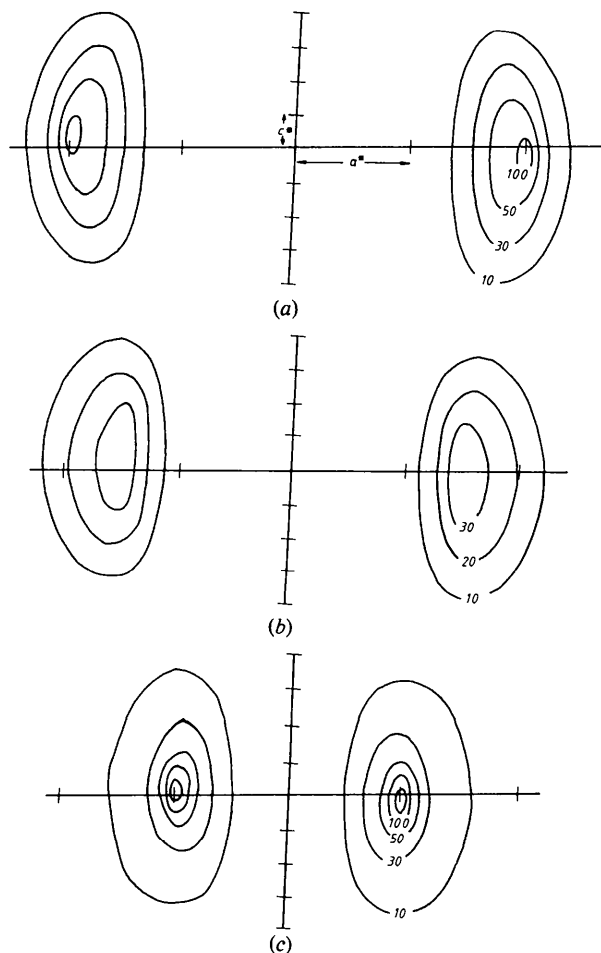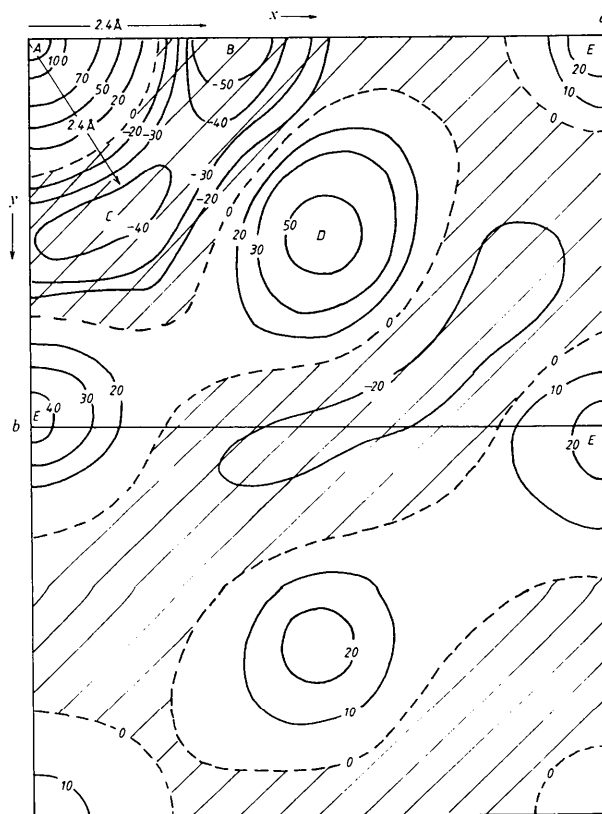Fig. 12. The Fourier transform of the diffuse scattering in the section of reciprocal space perpendicular to c^* passing through the origin. The contours are labelled in relative units.

In the proposed structure rotational isomerism occurs about three particular carbon–carbon bonds in the soap molecule. These bonds are approximately parallel to the inter-layer long spacing. The projections down the long spacing on to the ab plane of the three alternative configurations of the C(4)–C(5) segment of the hydrocarbon chain produced by conformational changes about bond C(3)–C(4) are given in Fig. 13. The average structure, assuming that each configuration is equally probable, is also given. The two-dimensional difference Q function for the situation represented by Fig. 13 is given in Fig. 14. This was evaluated by first calculating the difference Fourier transform

$$I_D(s) = \overline{|F(s)|^2} - \left|\overline{F(s)}\right|^2 \qquad (8)$$

and then Fourier transforming the function obtained in the same way as the experimental diffuse scattering.

The atomic scattering factor for carbon was taken from *International Tables for X-ray Crystallography* (1968). Each atom was given an isotropic temperature factor of $15 \cdot 0\ \text{Å}^2$. The two *gauche* conformations were taken to be symmetrically disposed at rotation angles of $\pm 120°$ from the *trans* conformation.

In Fig. 14 two negative peaks, X and Y, are clearly resolved at vector displacements from the origin corresponding to the interatomic vector displacements x and y in the average structure. Negative peaks corresponding to all the other vector displacements between disordered atoms in the average structure exist in the difference Q function and are related to X and Y by the centre of symmetry at the origin and by reflection in the a or b cell edges.

Figs. 15 and 16 give the average structure and difference Q function respectively produced by conformational disorder about three next-nearest-neighbour bonds (27 configurations). Peaks X and Y are again clearly resolved but have been displaced radially outwards from the origin relative to their position in Fig. 14. No peaks corresponding to the additional

Fig. 13. Alternative conformations about a single carbon–carbon bond in a hydrocarbon chain.

Fig. 15. Average structure in projection produced by conformational disorder about three next-nearest neighbour carbon–carbon bonds assuming equal weighting for each conformation.
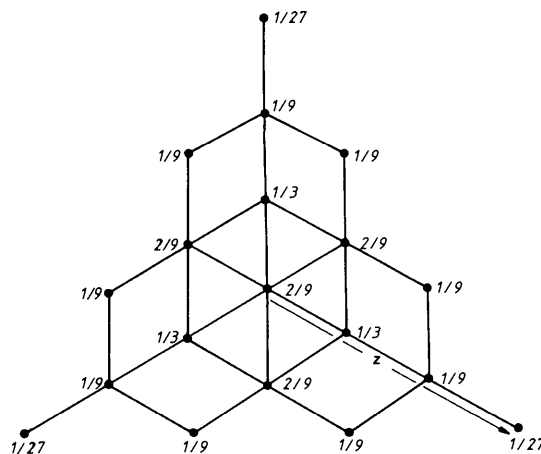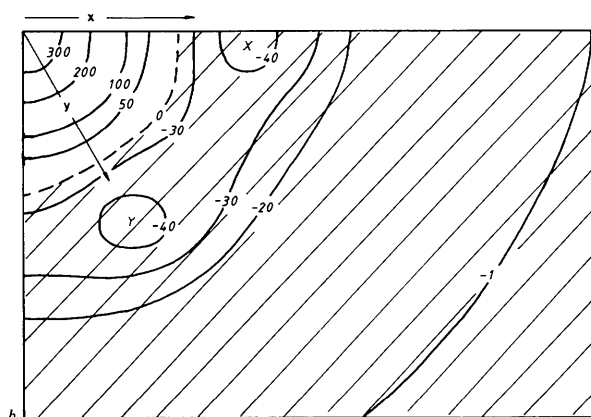

Fig. 14. The difference Q function of Fig. 13. Contours labelled in relative units.

Fig. 16. The difference Q function of Fig. 15.

interatomic vector displacements which exist in Fig. 15 (*e.g.* z) are resolved but overall the difference Q function of Fig. 15 is, as would be expected, more extensive than that of Fig. 13. The difference Fourier transform for the structure represented by Fig. 15 is given in Fig. 17. This corresponds to the diffuse scattering which would be observed from a system of molecules, disordered in the manner of Fig. 15 and arranged on a regular lattice with no correlation between the states of neighbouring molecules. The scattering is less localized than that observed experimentally.

It is suggested that the peaks B and C in the experimental difference Q function can be identified with the peaks X and Y of Fig. 16 and thus originate from interatomic displacements between the various configurations of a single molecule. Peak B is greater in magnitude than peak C suggesting that *gauche* 1–*gauche* 2 displacements are more numerous in the average structure than *gauche–trans* displacements. The positive peaks D and E of Fig. 12 do not appear in the difference Q function calculated for a single disordered molecule. These have been interpreted as arising from correlations between the states of neighbouring molecules. Intermolecular correlations also account for the localization of the diffuse scattering into diagonal streaks between particular reciprocal-lattice points.

Intermolecular correlations

In order to assess the influence of intermolecular correlations, a simplified model for the disordered structure has been examined. The disordered segments of chain pack on a pseudo-hexagonal lattice which has been defined by the lattice vectors $\mathbf{a}'$ and $\mathbf{b}'$ in Fig. 18. Packing models suggest that steric interactions are

strongest between molecules related by an $\mathbf{a}'$ or $\mathbf{b}'$ vector displacement. In the model which is developed, the order of 'neighbourhood' of two molecules is equal to the number of $\mathbf{a}'$ plus the number of $\mathbf{b}'$ vector displacements which connects them. On Fig. 18 first-nearest neighbours to the molecule 0 are labelled 1 and second-nearest neighbours 2. It is assumed that the states of molecules in different layers parallel to the ab plane are independent. The total diffuse scattering is then given by the product of the diffuse scattering from a single layer and the number of layers. It is further assumed that each molecule can adopt just two alternative configurations, A or B, with equal probability and that nearest-neighbour molecules in the same configuration, related to each other by the glide plane in the actual crystal, are related simply by the $\mathbf{a}'$ or $\mathbf{b}'$ translation of the $a'b'$ lattice [more detailed calculations in which this simplification is not made produce a similar result (Glover, 1977)]. Unit cells on the $a'b'$ lattice can therefore be said to be either type A or type B.

From (4) and (5) the diffuse scattering is given by

$$I_D(\mathbf{s}) = \mathrm{FT}\left(N\sum_m^{N'}\left\{\sum_i^n\sum_j^n P_i[\,p(ij\mathbf{u}_m) - P_j] \times Q_{ij}(\mathbf{r})\right\}\right.$$
$$\left. * \,\delta(\mathbf{r} - \mathbf{u}_m)\right). \tag{9}$$

For the case considered with just two types of unit cell

$$p(ii\mathbf{u}_m) = \tfrac{1}{2}(1 + C^{|w| + |w'|})$$

and

$$p(ij\mathbf{u}_m) = \tfrac{1}{2}(1 - C^{|w| + |w'|}),$$

where, if p is the probability that a first-nearest neighbour to the given molecule is of the same type, $C = 2p - 1$, and the integers w and w' are given by $\mathbf{u}_m = w\mathbf{a}' + w'\mathbf{b}'$.

With $P_i = P_j = \tfrac{1}{2}$ and expressing the real-space coordinates x' and y' in units of a' and b' and the

Fig. 17. The difference Fourier transform of Fig. 15. Contours labelled in relative units.

Fig. 18. Chain packing in C-phase KC_{10}. The pseudo-hexagonal lattice is defined by the vectors $\mathbf{a}'$ and $\mathbf{b}'$.

reciprocal-space coordinates H' and K' in units of the reciprocal-lattice spacing, we have

$$I_D(H', K') = \text{FT} \left\{ N \sum_w \sum_{w'} [(C^{|w| + |w'|} \, Q) \right.$$
$$\left. * \, \delta(x' - w, y' - w')] \right\}, \quad (10)$$

where

$$Q = \tfrac{1}{4}[Q_{AA}(\mathbf{r}) + Q_{BB}(\mathbf{r}) - Q_{AB}(\mathbf{r}) - Q_{BA}(\mathbf{r})] \quad (11)$$

and the summations are made over all possible values of w and w'. Q is identical to the difference Q function of the crystal with no correlations. Making use of the convolution theorem, we find that

$$I_D(H', K') = N(\text{FT} \, Q) \, \text{FT} \left[\sum_w \sum_{w'} C^{|w| + |w'|} \right.$$
$$\left. \times \, \delta(x' - w, y' - w') \right]. \quad (12)$$

Thus we have the result that the diffuse scattering from the crystal with correlations is the same as that from a crystal without correlations modulated by the function

$$[\text{FT} \, C^{|x'| + |y'|}] * \left[\text{FT} \sum_w \sum_{w'} \delta(x' - w, y' - w') \right]. \quad (13)$$

In this expression $|w|$ and $|w'|$ have been replaced by the continuous variables $|x'|$ and $|y'|$. This substitution is permissible when $p \geq 0.5$.

The second term of (13) is the reciprocal lattice of the $a' b'$ lattice as shown in Fig. 19. The first term may readily be evaluated as

$$\frac{4(\ln C)^2}{[4\pi^2 H'^2 + (\ln C)^2][4\pi^2 K'^2 + (\ln C)^2]}. \quad (14)$$

This function peaks at the origin where both H' and K' are zero simultaneously and extends more strongly from the origin in $a'*$ and $b'*$ directions, where either

H' or K' is zero, than in more general directions. The overall modulating function given by the convolution of (14) with the reciprocal lattice is illustrated schematically in Fig. 19.

Some illustrative calculations have been performed on the model given by Fig. 20. A single carbon atom is disordered between two sites displaced from each other by 2·4 Å parallel to the a unit-cell edge. This is the situation which would result from conformational disorder about a single carbon–carbon bond with zero probability of a *trans* conformation occurring. The difference Fourier transform (the diffuse scattering) and difference Q function with $p = 0.5$ (no correlations) are given in Fig. 21. The effect of correlations is shown in Fig. 22 calculated for $p = 0.75$. Correlations result in the concentration of the diffuse scattering about the points 11 and 20 and along the line connecting them. Thus, whatever the nature of the disorder of a single molecule, provided the difference Fourier transform is relatively strong in the region of these reciprocal-lattice points, correlations of the type considered will result in diffuse scattering distributed as observed experimentally.

The interatomic vector displacements producing the peaks B', C', D', E' and F' in Fig. 22(b) are shown by the vectors 1, 2, 3, 4 and 5 on Fig. 20. Comparison of Fig. 22(b) with the experimental difference Q function

Fig. 20. The average structure of the simple disordered model which was examined in order to assess the effect of intermolecular correlations on the diffuse scattering.
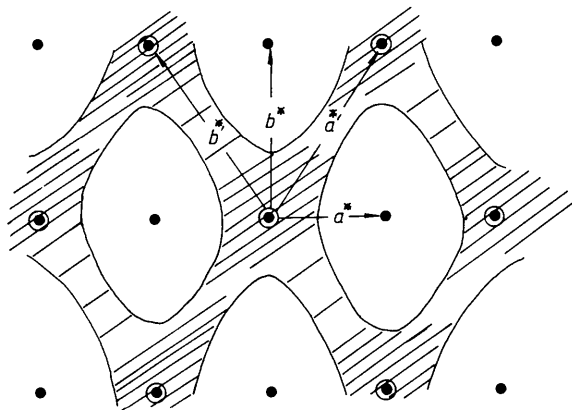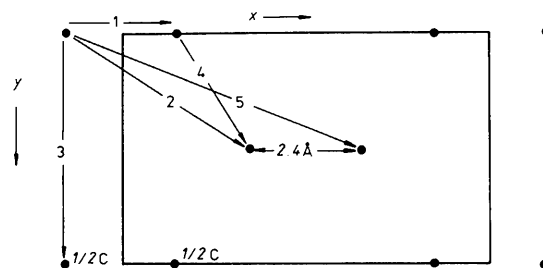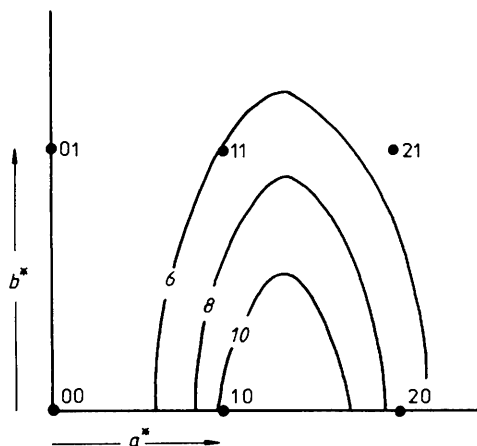

Fig. 19. The reciprocal lattice of Fig. 18, showing schematically the form of the function which modulates the diffuse scattering as a result of intermolecular correlations. O Reciprocal-lattice point on the $a'*b'*$ lattice; ● reciprocal-lattice point on the $a*b*$ lattice; /// modulating function.

Fig. 21. The difference Fourier transform of Fig. 20; $p = 0.5$.

(Fig. 12) suggests that the positive peaks D and E result, as does the diffuse streaking, from intermolecular correlations. The relative heights of these peaks indicate that correlations are strongest between molecules related by the glide plane. Molecules related by the translation **b** are more strongly correlated than those related by **a** or **a** + **b** translations. The negative peak C' in the model calculations does however demonstrate a source of ambiguity in the interpretation of the experimental results. It results from an intermolecular interatomic displacement of 3·3 Å which has a low weight in the real crystal due to steric hindrance but exists with full weight in the average crystal. Similar peaks may contribute to the negative regions B and C of Fig. 12 and it is therefore not safe to conclude that these two peaks result entirely from intramolecular interatomic displacements.

Fourier transformation of the full, three-dimensional distribution of diffuse scattering would give the three-dimensional difference Q function of the crystal. By inspection of Figs. 10 and 11 this would be concentrated in the ab plane of real space. The transformation was not performed quantitatively as it was considered that it would provide no additional information about the nature of the disorder.

Discussion

Although their origin cannot be determined unambiguously, the presence of the negative peaks B and C in the difference Q function gives strong support to the proposal that disorder between *trans* and *gauche* conformations occurs about particular carbon–carbon bonds. The peak B in particular corresponds well to the existence of an interatomic inter-configuration displacement of 2·4–2·8 Å parallel to the a cell edge. This is the displacement which relates the disordered segments of the two rotational isomers which can be produced by the introduction of a $2g1$ kink in the chain.

Packing considerations dictate that the conformation of neighbouring molecules must be correlated. The existence of such correlations is indicated by the presence in the difference Q function of positive peaks at vector displacements from the origin corresponding to lattice vectors. Model calculations demonstrate that the effect of correlations on the diffuse scattering is to concentrate it about, and along the lines connecting, reciprocal-lattice points. It should be noted however that the modulating function of Fig. 19 is that for a much simplified model with just two alternative unit cells as opposed to up to 27 for the proposed disorder mechanism; but it is at least plausible that the diffuse scattering will be modulated in a similar way by correlations in the real system.

Modulation of the difference Fourier transform given in Fig. 17 by the function in Fig. 19 would produce the prominent band of diffuse intensity observed to join 110 and 200 (and equivalents). This modulating function also contains a band joining 110 (and its equivalent) to the origin and there is appreciable intensity present in this region of the function to be modulated. No diffuse intensity was observed along this line. This apparent inconsistency may be accounted for in part by the fact that the difference Fourier transform of Fig. 17 was calcualted giving equal weighting to each of the 27 alternative chain configurations. As discussed, both packing considerations and the experimental difference Q function suggest that kinked chain configurations with two or three *gauche* bonds are more numerous than the more extended all-*trans* and one *gauche* configurations. Differences in the weightings of alternative configurations in the actual crystal may be such as to reduce the diffuse intensity along the line considered. However, even in the case of the model given in Fig. 20, in which there are only *gauche–gauche* displacements, the difference Fourier transform given by Fig. 22(*a*) still contains some extension of the diffuse intensity from 110 along the line to the origin. This discrepancy thus remains to be fully resolved.
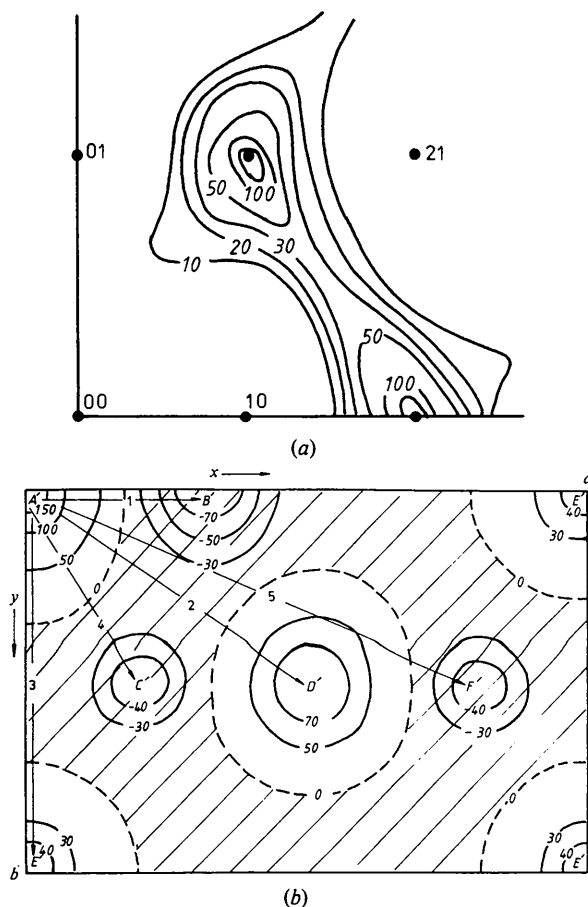

Fig. 22. The difference Fourier transform (*a*) and the difference Q function (*b*) of Fig. 20; $p = 0.75$.

Conclusions

On the basis of the electron density distribution, derived from Lewis's Bragg diffraction data, in conjunction with considerations of molecular geometry and packing, it is proposed that the hydrocarbon chains in C-phase potassium caprate are partially disordered.

At the A to C transition a cooperative 'melting' of the chains apparently takes place involving the introduction of *gauche* conformations about particular carbon–carbon bonds. The extent of the chain melting is restricted by the fact that the ionic groups maintain an ordered layered structure thus limiting the cross-sectional area available per molecule in planes perpendicular to the long spacing.

This model is consistent with available thermodynamic data and with the majority of the features of the diffuse X-ray scattering observed from single crystals.

The author is indebted to the late T. R. Lomer for his greatly valued support, advice and criticism throughout the course of this work.

APPENDIX
Extrapolation of the experimental diffuse scattering to the Bragg positions

In order to estimate the diffuse intensity at and immediately adjacent to reciprocal-lattice points it was assumed that, in comparison to the modulating function resulting from correlations, in the vicinity of a lattice point the molecular Fourier transform varies only slowly with distance from that point.

With this approximation the diffuse intensity near a lattice point for the model developed in equations (9) to (14) above is given by

$$I_D(H', K') = \frac{k4(\ln C)^2}{[4\pi^2 H'^2 + (\ln C)^2][4\pi^2 K'^2 + (\ln C)^2]}$$

$$(A1)$$

where k is a constant and H' and K' are now displacements from the point in the $\mathbf{a'^*}$ and $\mathbf{b'^*}$ directions respectively.

Along the line connecting 110 and 200 where K' is zero ($A1$) reduces to

$$I_D(H') = \frac{k4(\ln C)^2}{[4\pi^2 H'^2 + (\ln C)^2]k'} = \frac{A}{BH'^2 + D}, \quad (A2)$$

where k', A, B and D are constant. Plots of H'^2 *versus* $1/I_D(H')$ for the experimental data in the vicinity of the points 200 and 110 produced straight lines which were

extrapolated to obtain estimates of the diffuse intensity at these points.

References

AMORÓS, J. L. & AMORÓS, M. (1968). *Molecular Crystals: their Transforms and Diffuse Scattering.* New York: John Wiley.

BUERGER, M. J. (1962). *Z. Kristallogr.* **117**, 358–361.

COCHRAN, W. (1956). *Acta Cryst.* **9**, 259–262.

DUMBLETON, J. H. (1964). *Crystal Structure and Phase Transformations in Potassium Soaps.* Thesis, Univ. of Birmingham.

FLORY, P. J. (1969). *Statistical Mechanics of Chain Molecules.* New York: Wiley Interscience.

GALLOT, B. & SKOULIOS, A. (1966a). *Kolloid Z. Z. Polym.* **209**, 164–169.

GALLOT, B. & SKOULIOS, A. (1966b). *Kolloid Z. Z. Polym.* **210**, 143–149.

GALLOT, B. & SKOULIOS, A. (1966c). *Mol. Cryst. Liq. Cryst.* **1**, 263–292.

GALLOT, B. & SKOULIOS, A. (1968). *Kolloid Z. Z. Polym.* **213**, 143–150.

GLOVER, D. M. (1977). *The Molecular Basis of Structural Phase Transitions in Potassium Soaps.* Thesis, Univ. of Birmingham.

GLOVER, D. M. & LOMER, T. R. (1979). *Mol. Cryst. Liq. Cryst.* **53**, 181–188.

GRANT, R. F. & DUNELL, B. A. (1960). *Can. J. Chem.* **38**, 1951–1956.

GRANT, R. F. & DUNELL, B. A. (1961). *Can. J. Chem.* **39**, 359–362.

GRAY, G. W. & WINSOR, P. A. (1974). *Liquid Crystals and Plastic Crystals.* Chichester: Ellis Harwood.

HOSEMANN, R. & BAGCHI, S. N. (1962). *Direct Analysis of Diffraction by Matter.* Amsterdam: North-Holland Publishing Co.

International Tables for X-ray Crystallography (1968). Vol. III, 2nd ed. Birmingham: Kynoch Press.

JANZEN, W. R. & DUNELL, B. A. (1962). *Can. J. Chem.* **40**, 1260–1265.

KITAIGORODSKY, A. I. (1957). *Organic Chemical Crystallography.* New York: Consultants Bureau.

LEE, A. G. (1975). *Prog. Biophys. Molec. Biol.* **29** (1), 5–56.

LEWIS, E. L. V. (1967). *An X-ray Investigation of the Structure of Potassium Caprate.* Thesis, Univ. of Birmingham.

LEWIS, E. L. V. (1968). Unpublished report to Unilever Ltd.

LEWIS, E. L. V. & LOMER, T. R. (1969). *Acta Cryst.* B**25**, 702–710.

LOMER, T. R. (1952). *Acta Cryst.* **5**, 11–14.

LOMER, T. R. (1977). Private communication.

MATSUBARA, T. (1952). *J. Phys. Soc. Jpn*, **7**, 270–274.

SKOULIOS, A. & LUZZATI, V. (1961). *Acta Cryst.* **14**, 278–286.

WILSON, A. J. C. (1962). *X-ray Optics*, 2nd ed. London: Methuen.

ZACHARIASEN, W. H. (1945). *Theory of X-ray Diffraction in Crystals.* New York: John Wiley.